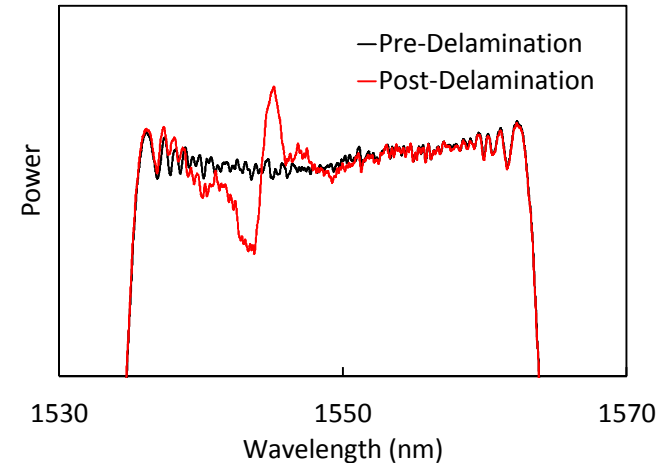
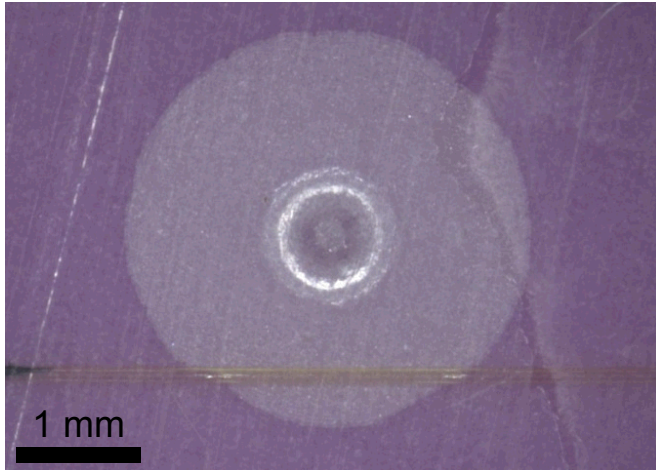


Exceptional service in the national interest



Sensing delamination in epoxy encapsulant systems with fiber Bragg gratings

Brad H. Jones, Garth D. Rohr, Amy K. Kaczmarowski

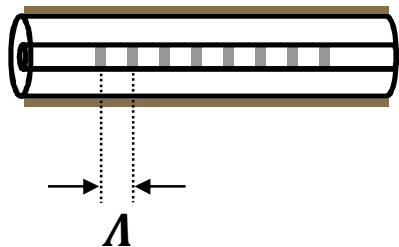
April 21, 2016

Fiber Bragg Gratings

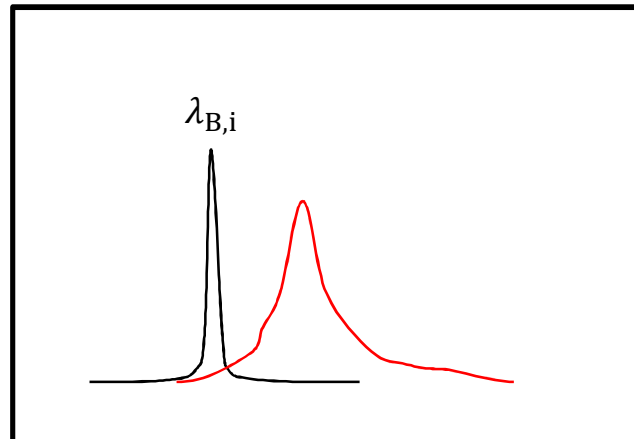
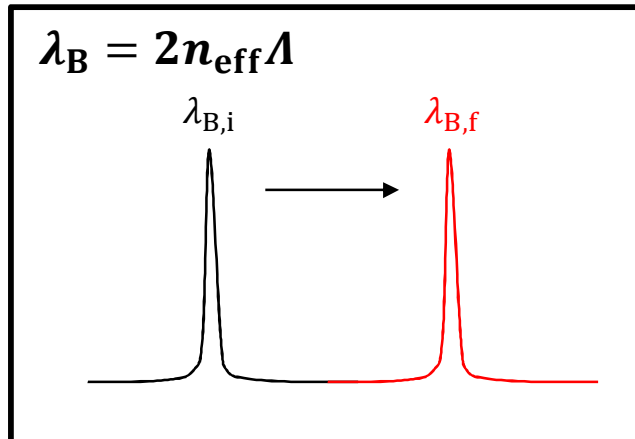
under uniform strain:

under non-uniform strain:

Uniform FBGs



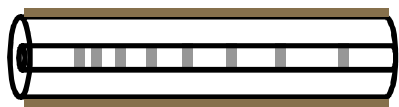
Reflected Power



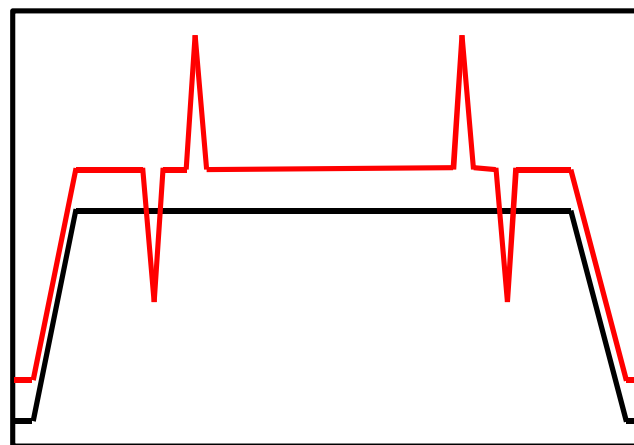
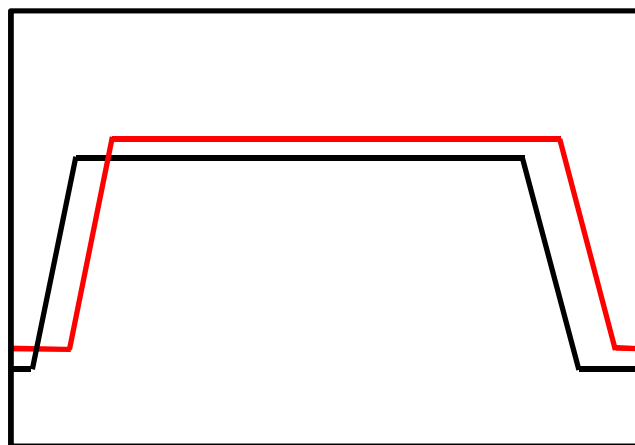
Wavelength

Wavelength

Chirped FBGs



Reflected Power

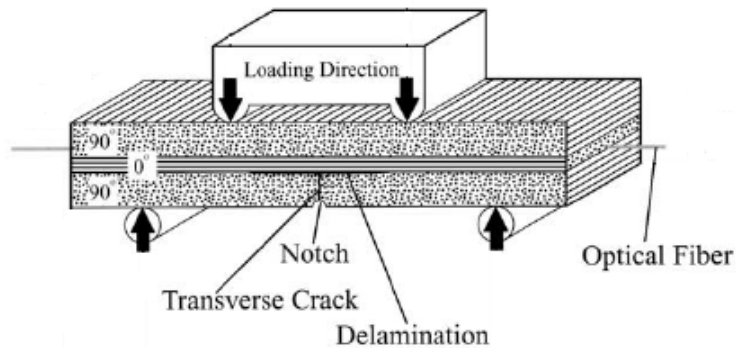


Wavelength

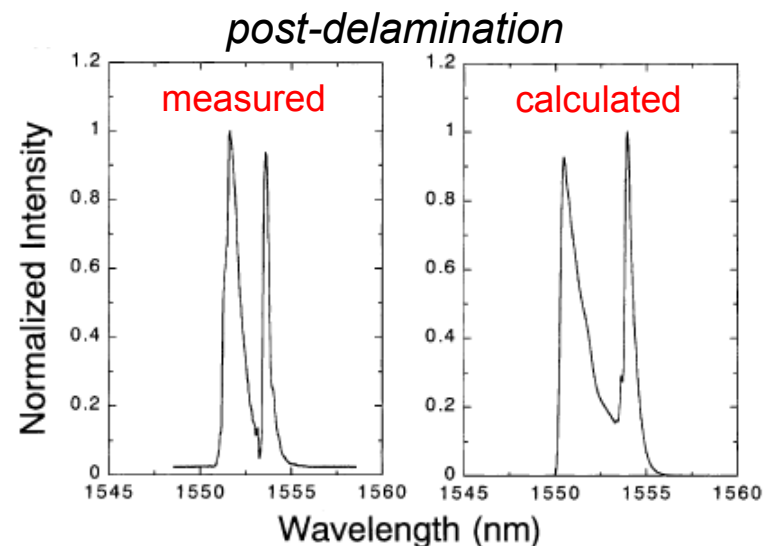
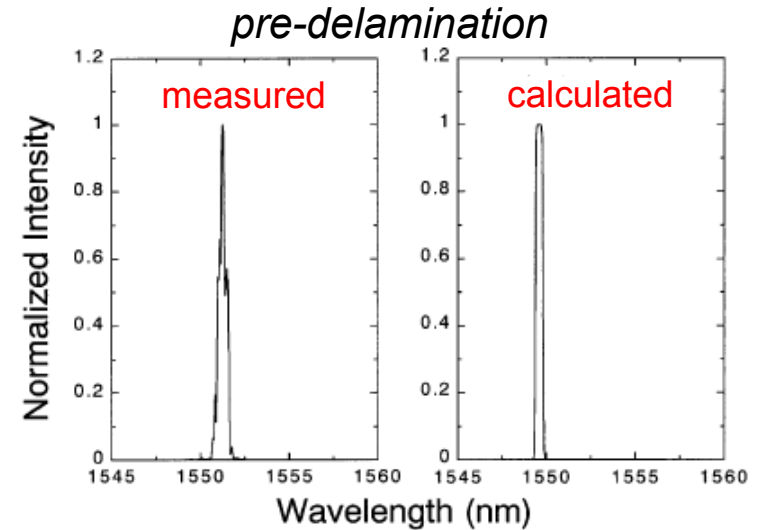
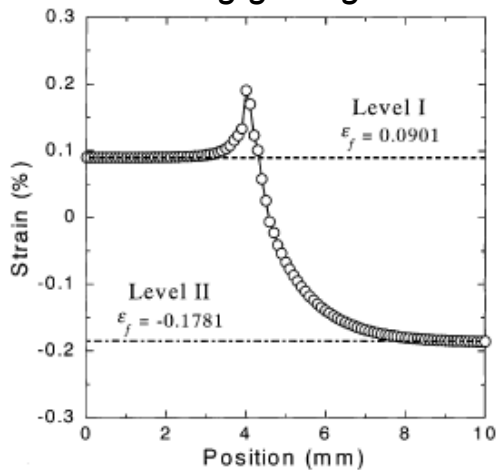
Wavelength

Fiber Bragg Gratings and Delamination

Past work with fiber-reinforced composites has shown non-uniform FBG axial strain distributions associated with delamination

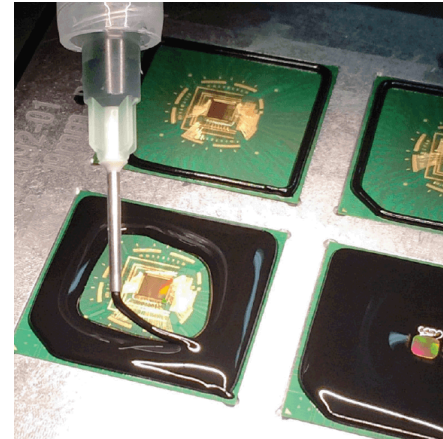


FEM-predicted strain distribution along grating



Our Objectives

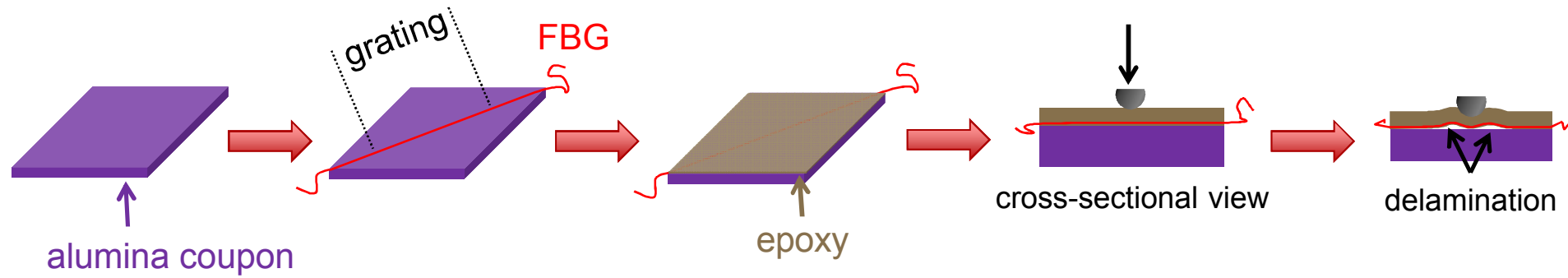
Many encapsulated devices are at high risk for internal delamination that can only be diagnosed by device failure!



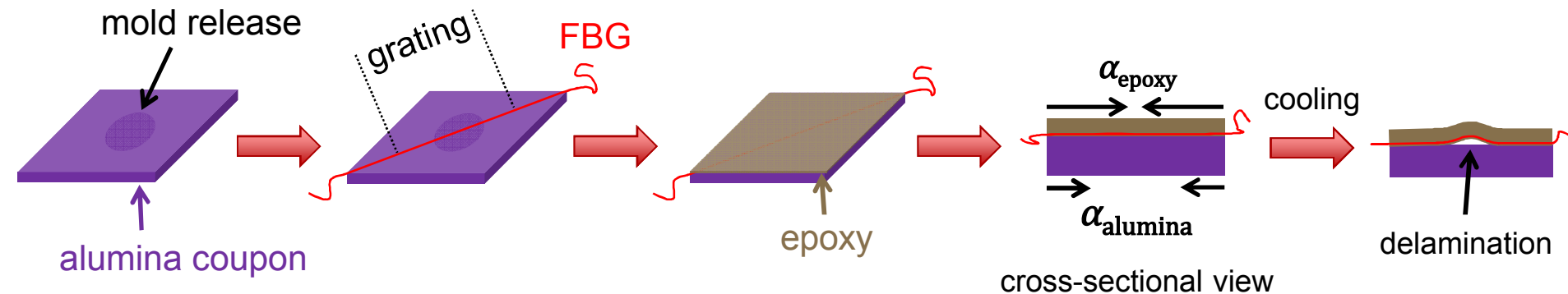
<http://www.samtecmicroelectronics.com>,
retrieved Nov. 2015

- **Can we use embedded FBGs to passively sense the occurrence of delamination at interfaces between encapsulants and their encapsulated materials?**
 - **What are the local strain profiles associated with delamination?**
 - **Can we correlate FBG response with key interfacial properties (e.g., delamination size, adhesive strength)**
- **Can we use embedded FBGs in complex and functional encapsulated devices to provide an indication of delamination-associated failure?**

Method 1: Indentation-Induced Delamination



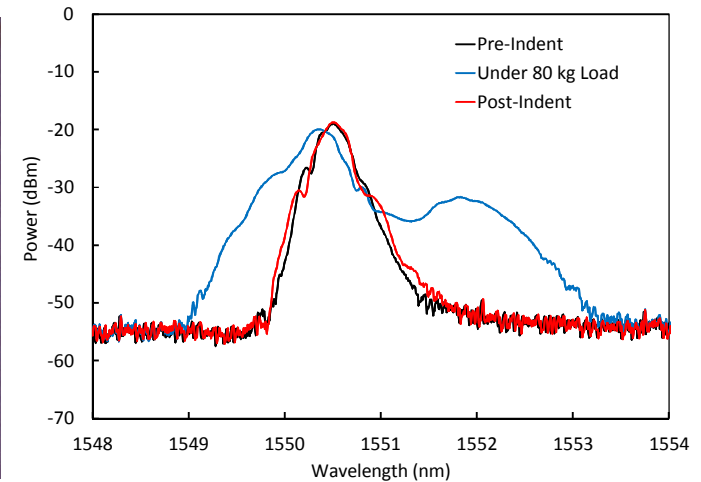
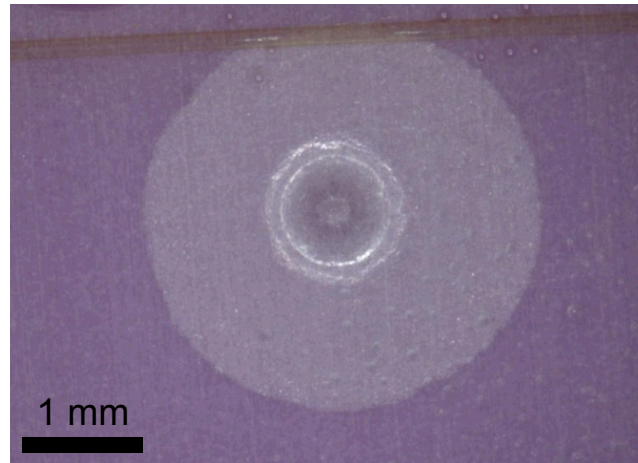
Method 2: Thermal Mismatch-Induced Delamination



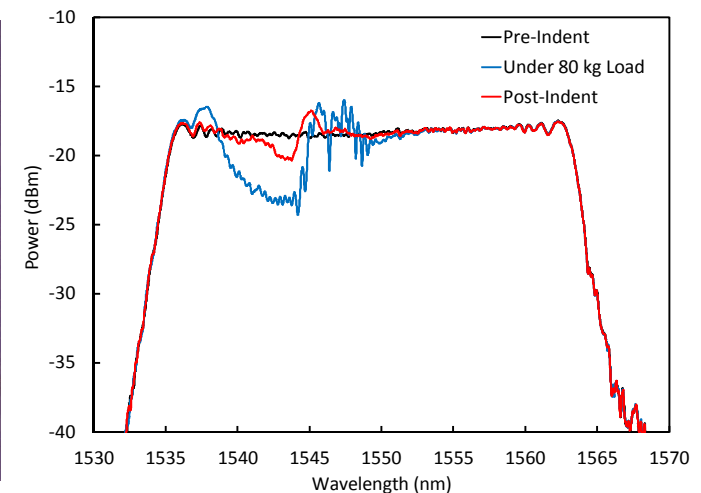
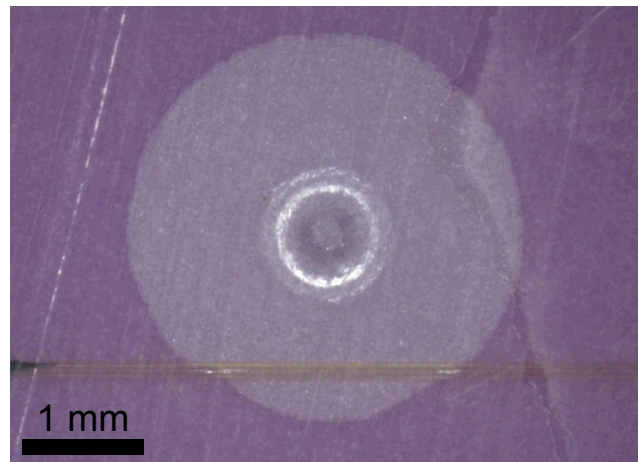
Indentation-Induced Delamination

Embedded FBGs exhibit characteristics of non-uniform strain distribution during and after indentation and delamination

Uniform FBG



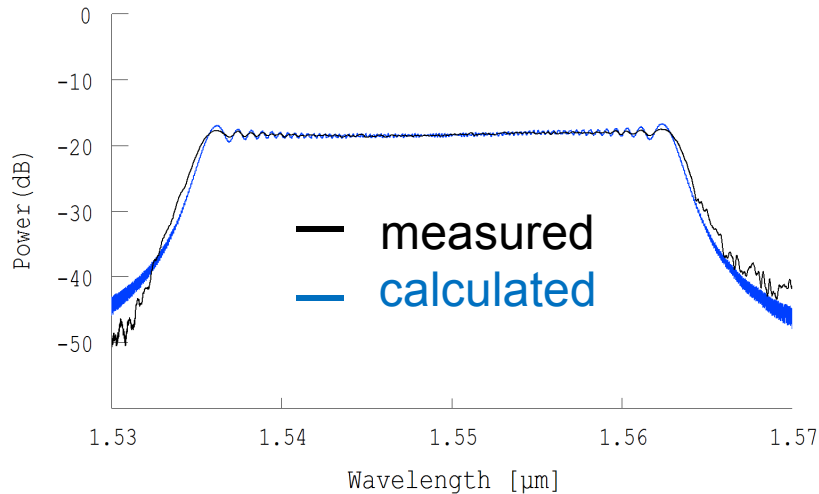
Linearly Chirped FBG



Residual Strain Distribution

OptiGrating simulation qualitatively captures residual perturbation in chirped spectrum using a Gaussian tensile strain distribution

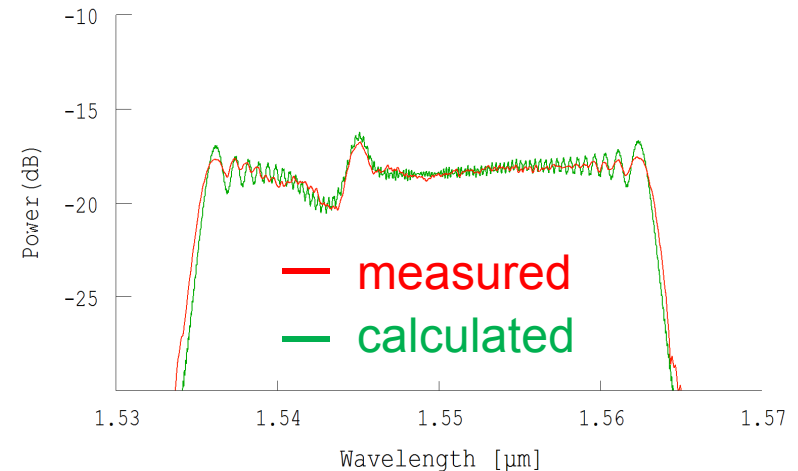
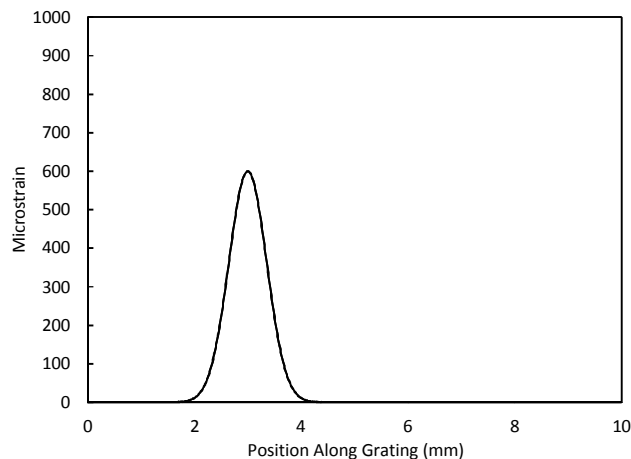
Pre-Indent



OptiGrating Inputs

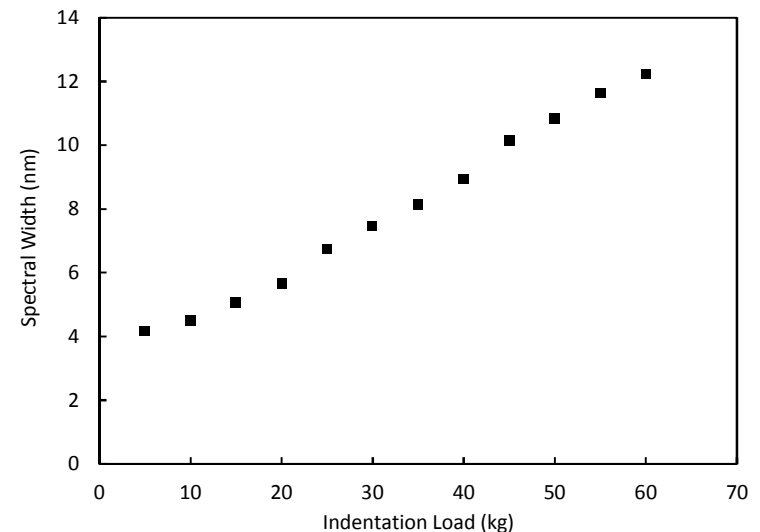
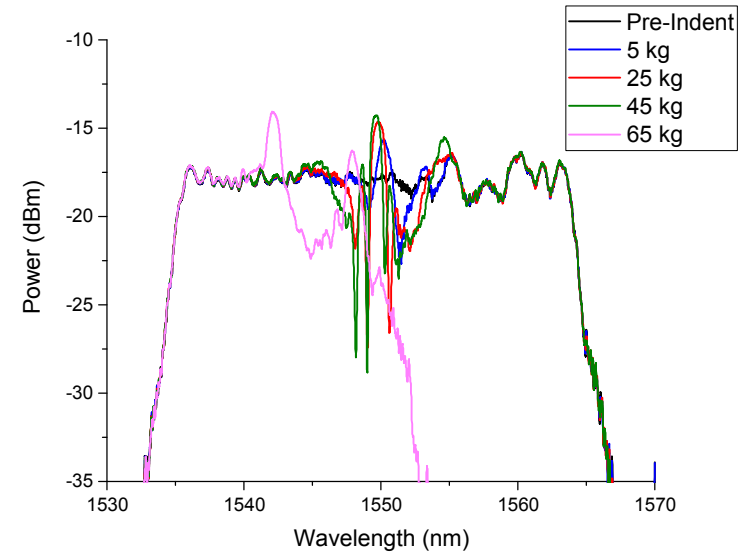
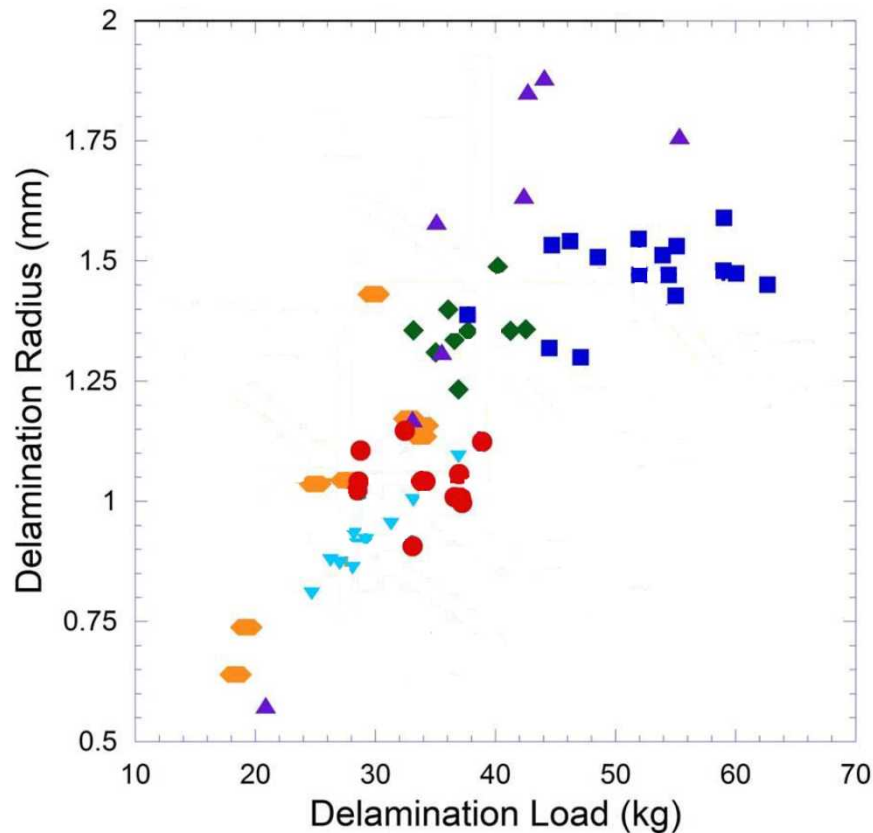
- Core-cladding refractive indices (RIs) and dimensions of SMF-28 standard
- Sinusoidal core RI variation $1.15 \cdot 10^{-4}$
- 10 mm grating length
- 10 nm linear chirp function
- Center wavelength 1549.3 nm

Post-Indent



Indentation Load Scaling

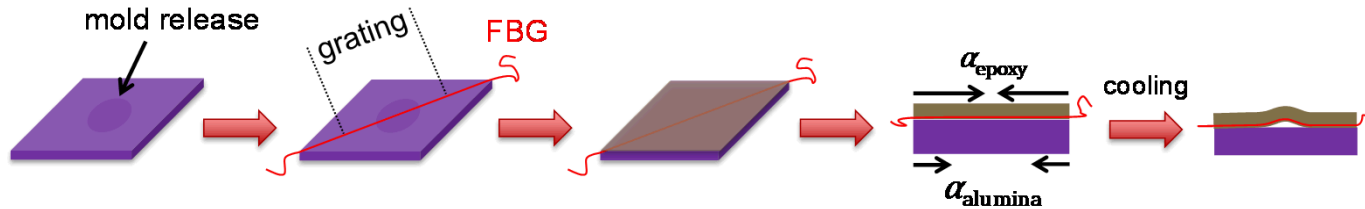
The width over which a given spectrum deviates from its corresponding spectrum pre-indentation scales with indentation load



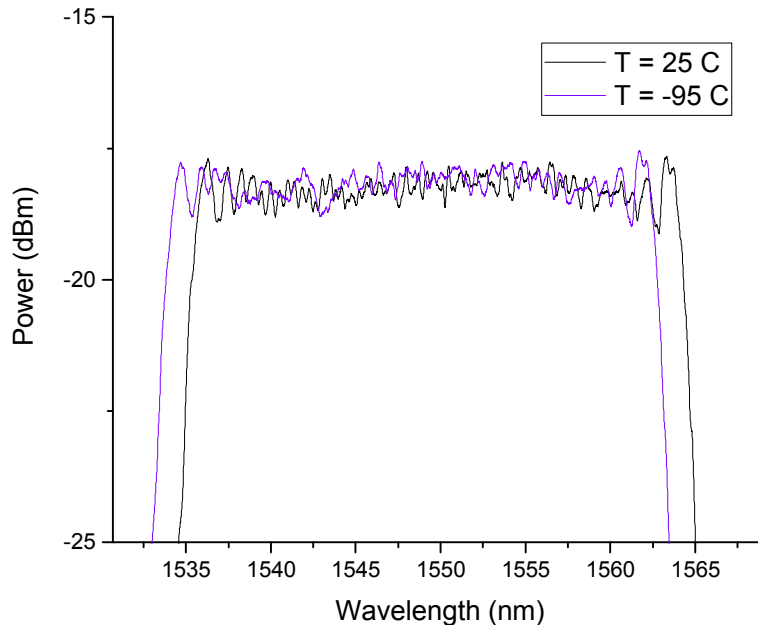
Adapted from K.I. Hutchins, *M.S. Thesis*, University of New Mexico **2015**.

Thermally-Induced Delamination

Embedded FBGs exhibit characteristics of non-uniform strain distribution concomitant with delamination

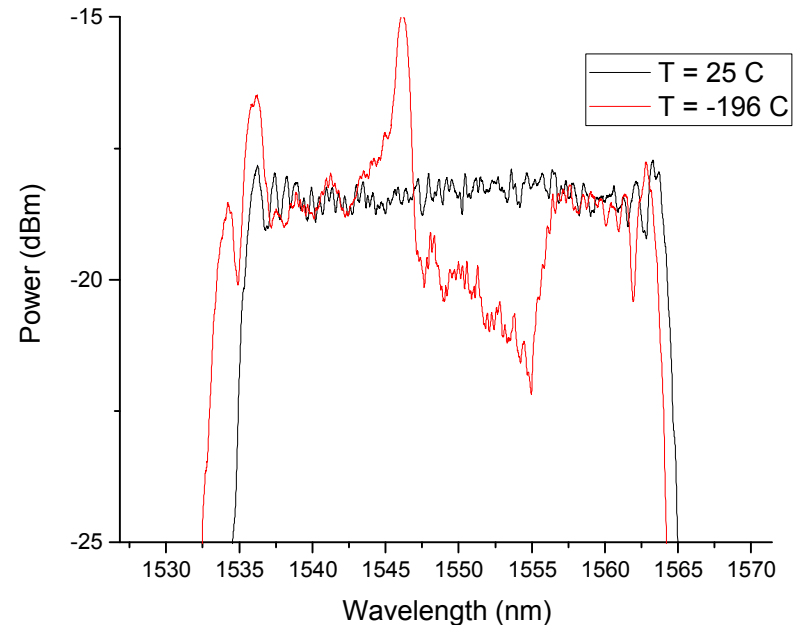


Cooling to $-95\text{ }^{\circ}\text{C}$: No delamination



spectra indicate a uniform strain profile across the grating

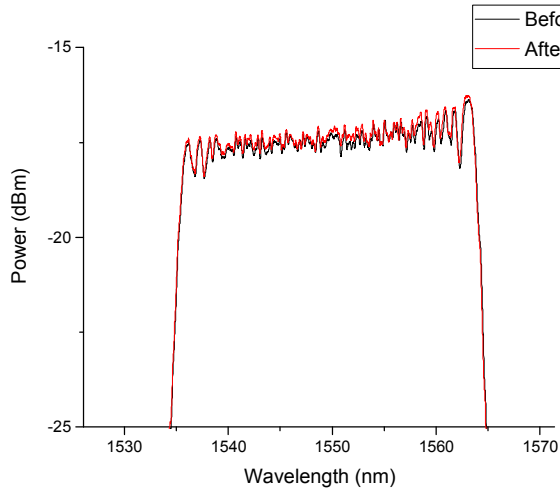
Cooling in LN_2 ($-196\text{ }^{\circ}\text{C}$): Clear delamination



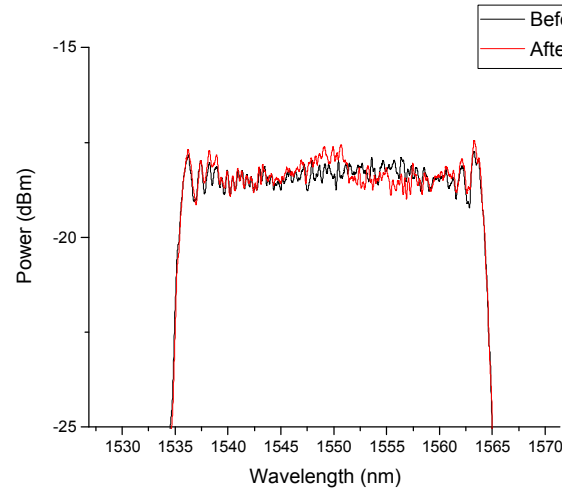
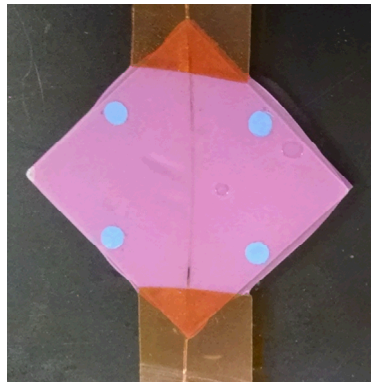
spectra indicate the development of a non-uniform strain distribution across the grating

Thermally-Induced Delamination

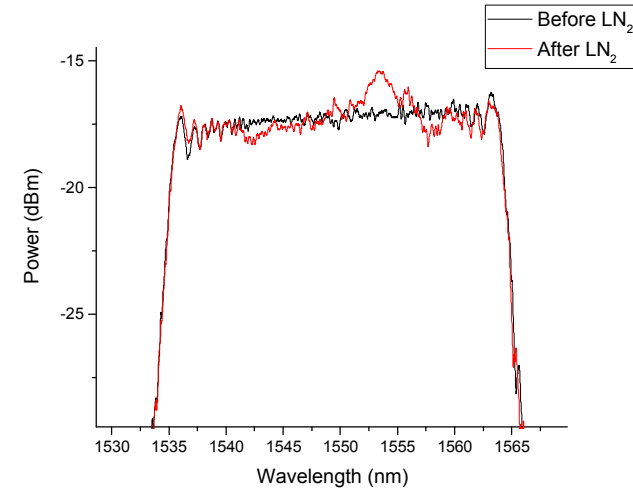
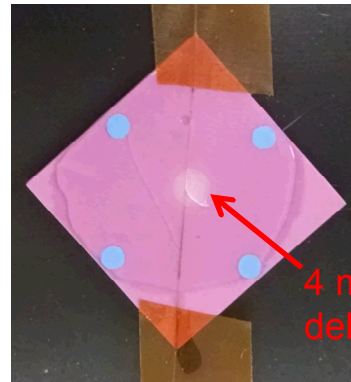
Again, the width over which a given spectrum deviates from its pre-delaminated spectrum is connected to delamination size



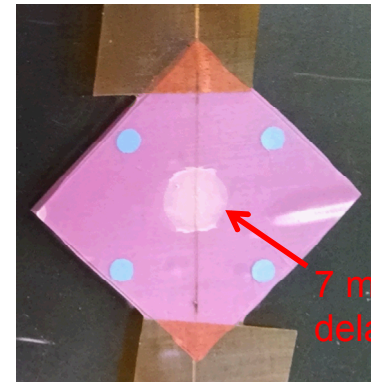
no mold release



0.5 μL mold release

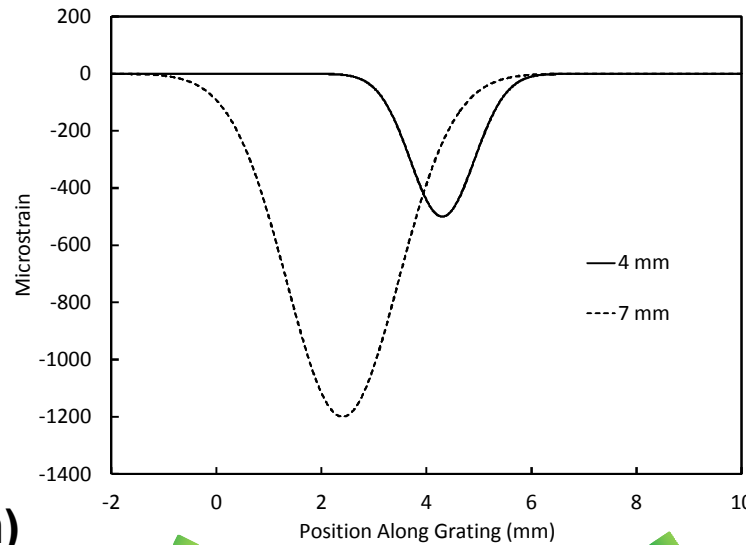


1.0 μL mold release

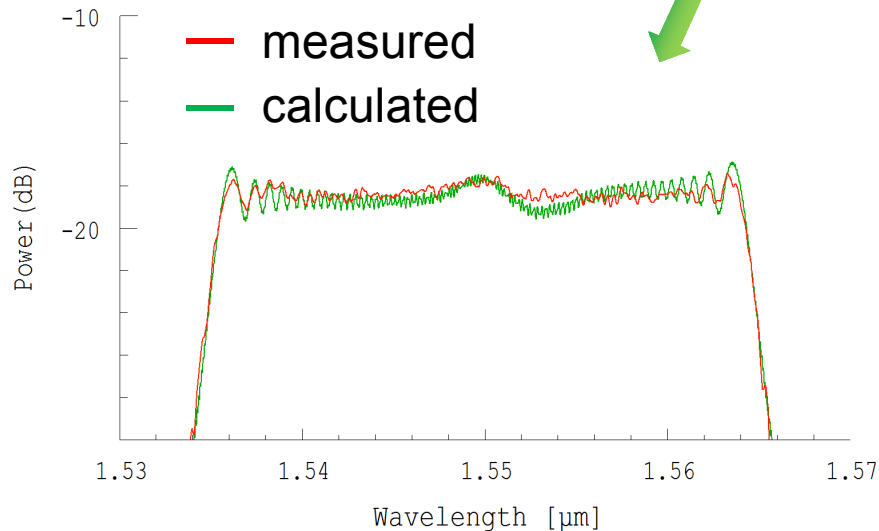


Residual Strain Distributions

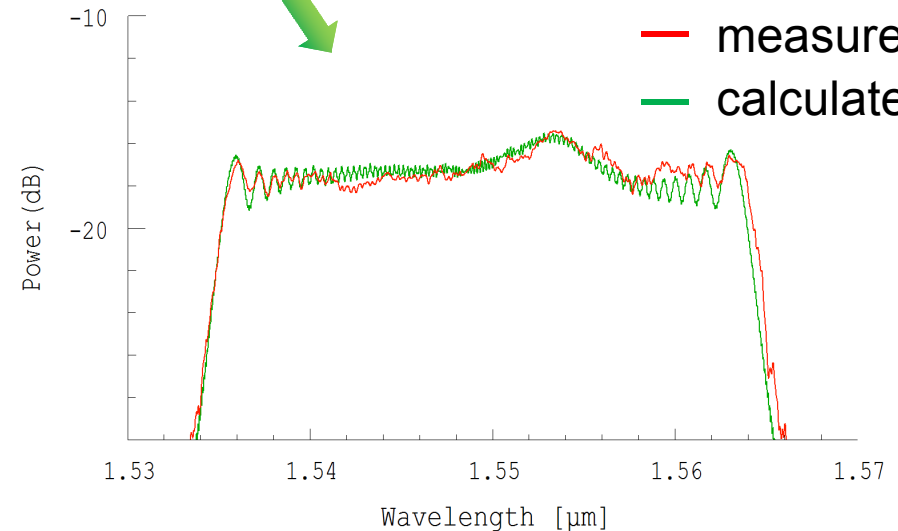
OptiGrating simulation roughly captures residual perturbation in chirped spectra using a Gaussian compressive strain distribution



0.5 μL MR (4 mm delam)



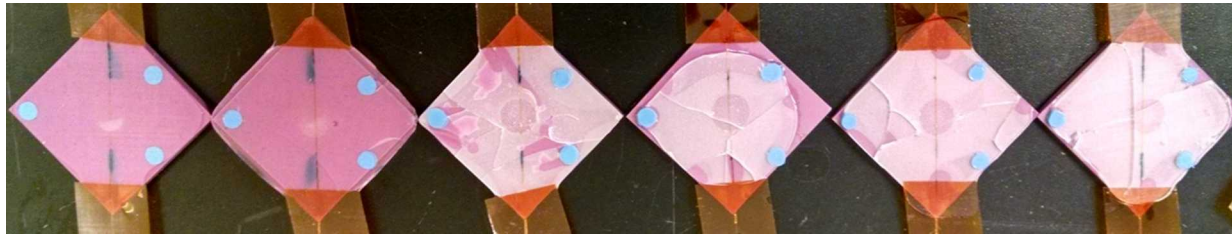
1.0 μL MR (7 mm delam)



Challenges in Scale

Cracking processes (including delamination) are activated at smaller temperature excursions as we move from film to bulk geometries

epoxy films of variable thickness cooled to $-196\text{ }^\circ\text{C}$

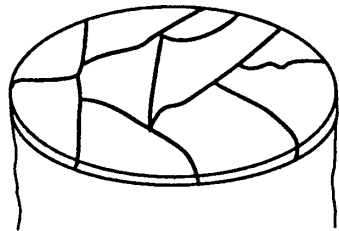


413 μm



1320 μm

channeling



delamination



$$\Omega = \frac{(1 - \nu_f)\sigma^2 h}{E_f}$$

$\Omega \equiv$ stored strain energy

$G \equiv$ strain energy release rate

$$G = \frac{Z\sigma^2 h}{E_f}$$

$h \equiv$ thickness

$Z \equiv$ driving force

$$\sigma = \frac{(\alpha_f - \alpha_s)\Delta T \cdot E_f}{1 - \nu_f}$$

$\alpha_f \equiv$ film CTE

$\alpha_s \equiv$ substrate CTE

$T \equiv$ temperature

$E_f \equiv$ film modulus

Conclusions

- **Chirped FBGs embedded in epoxy encapsulants provide readily identifiable spectral signatures in response to delamination**
- **Spectral analysis suggests residual Gaussian axial strain distributions in embedded FBGs after indentation- and thermally-induced delamination**
- **Key spectral features scale with delamination dimensions**

Future Directions

- **Implementation of genetic algorithm methods for strain calculations**
- **Extend to filled encapsulants**
- **Extend to bulk, complex geometries**

Acknowledgements

- **Clay Newton and Thomas Buchheit** – indentation instrumentation
- **Thomas Buchheit, David Reedy, Patricia Sawyer, Mark Stavig, Eric Udd** – discussion and experimental support